



**HAL**  
open science

## Evolution of the daytime atmospheric boundary layer structure in a deep Alpine valley

Charles Chemel, Jean-Pierre Chollet, Guillaume Brulfert, Eric Chaxel

### ► To cite this version:

Charles Chemel, Jean-Pierre Chollet, Guillaume Brulfert, Eric Chaxel. Evolution of the daytime atmospheric boundary layer structure in a deep Alpine valley. 16th Symposium on boundary layers and turbulence, Aug 2004, Portland, United States. hal-00203463

**HAL Id: hal-00203463**

**<https://hal.science/hal-00203463v1>**

Submitted on 29 Mar 2020

**HAL** is a multi-disciplinary open access archive for the deposit and dissemination of scientific research documents, whether they are published or not. The documents may come from teaching and research institutions in France or abroad, or from public or private research centers.

L'archive ouverte pluridisciplinaire **HAL**, est destinée au dépôt et à la diffusion de documents scientifiques de niveau recherche, publiés ou non, émanant des établissements d'enseignement et de recherche français ou étrangers, des laboratoires publics ou privés.



Distributed under a Creative Commons Attribution 4.0 International License

## P4.6 EVOLUTION OF THE DAYTIME ATMOSPHERIC BOUNDARY LAYER STRUCTURE IN A DEEP ALPINE VALLEY

Charles Chemel\*, Jean-Pierre Chollet, Guillaume Brulfert and Eric Chaxel  
Laboratoire des Ecoulements Géophysiques et Industriels, UJF-CNRS-INPG, Grenoble, France

### ABSTRACT

High-resolution numerical simulations using the ARPS (Advanced Regional Prediction System) model have been compared with collected data during a whole week of POVA field campaign in the Maurienne valley (France) during summer 2003. Wind profiler and tethered balloon were operated to investigate vertical flow structure of the atmosphere and its evolution. Both ground surface and upper-levels calculated winds show good agreement with the observations. Specific features such as wind reversal and mixed boundary layer up to approximately the altitude of the surrounding mountains were reproduced. The wind reversal was observed to be much more sudden than in the Chamonix valley (France).

### 1. INTRODUCTION

Alpine valley are particularly sensitive to air pollution due to emission sources generally concentrated close to the valley floor and local meteorology induced by complex terrain. The program POVA ('Pollution des Vallées Alpines') was launched in May 2000. The main objective of the POVA program is to characterize the pollution sources and study the relationship between atmosphere dynamics and pollution events in the Chamonix and Maurienne valleys (France). This study benefits from an exceptional context, with the 'Tunnel du Mont Blanc' (TMB) in the Chamonix valley being closed for nearly 3 years after a large accident in March 1999. Most of the traffic, especially heavy duty traffic was transferred from the Chamonix valley to the Maurienne valley as long as the TMB was close. Therefore the program includes several intensive field campaigns, associated with 3D modeling before and after the reopening of the TMB.

Dynamical issues in mountainous areas has been discussed in numerous studies. Thermally driven winds in wide valleys are well documented, and Whiteman (1990) gives an overview of knowledge on the meteorological aspects. A stable nocturnal boundary layer forms at the surface at night when air temperature near the ground decreases in response to the radiational cooling of the surface. This process produces a shallow inversion and stable conditions, which reduces vertical mixing, thus confining surface-based pollutants to the lowest few hundred meters. Processes leading to temperature inversion breakup exert an important influence on the vertical transport and mixing of pollutants. Pollutants trapped in the stable atmospheric boundary layer during nighttime are

caught in the growing convective boundary layer (CBL). CBL develops from the valley floor and sidewalls due to surface heating. Thermally-generated upslope flows bring pollutants along the slopes and may dilute them at larger scale.

The Chamonix and Maurienne valleys significantly differs one another in shape, length, orientation and pollutant emissions. Results from the Chamonix valley were given in previous paper (Chemel *et al.*, 2004) when the Maurienne valley is considered hereafter. Some results from the Chamonix valley will be recalled in order to be compared to results from the Maurienne valley.

During the POVA observation periods, the CBL structure and its evolution was investigated using a UHF radar profiler. Beside measuring winds, the radar profiler also measured reflectivity, which can be used to compute the refractive index structure parameter  $C_n^2$ . This parameter measures fluctuations in the refractive index of the atmosphere and can be a very useful parameter for estimating the CBL height. Further details were presented in the Chamonix valley study (Chemel *et al.*, 2004). Due to ground clutter and atmospheric echoes, radar profilers are often blind close to the surface. To describe the lower layers of the atmosphere, the wind profiler was combined with a tethered balloon to provide full vertical profiles.

The objective of the experiment was to catch the local mixing depth structure and its evolution in the Chamonix and Maurienne valleys. A peculiar emphasis was put on transition periods in the morning and at twilight to give a better understanding of the growth and decay of the CBL.

Numerical simulations were compared with the POVA field data collected in winter and summer 2003. Large eddy simulation approach has been used to investigate local dynamics in both valleys. In the present paper, analyses and validation were performed for the last POVA field campaigns. This study will focus on the whole week

---

\* Corresponding author address: Charles Chemel, LEGI, BP 53 X, 38041 Grenoble, France; e-mail: Charles.Chemel@hmg.inpg.fr.

of observation in the Maurienne valley during summer 2003. The ARPS (Advanced Regional Prediction System) model developed at the University of Oklahoma was used with several grid nesting levels. The Maurienne valley was finally resolved on a 75 E-W by 63 N-S grid with spacings of 1 km  $\times$  1 km in the horizontal directions. This grid is coarser than the one used for the Chamonix valley because of a larger domain. The Chamonix valley was resolved on a 93 E-W by 103 N-S grid with a 300 m resolution. Results from ARPS were input afterwards in the meso-scale chemical-transport model TAPOM (Brulfert *et al.*, 2003).

## 2. OBSERVATIONAL SITE

The present study refers to the Maurienne valley in the French Alpine region. The topography of the region (Figure 1) is composed of various valleys of different shapes, lengths and orientation that makes the assessment of the air flow especially challenging. The Chamonix valley (site **A**) runs from southwest to northeast for about 15 km, is over 2000 m deep in average. The altitude of the highest mountain of the southeast mountain ridge (the Mont-Blanc) is 4810 m a.s.l. The peak-to-peak wavelength is about 4 km and the width of the valley bottom is about 1.5 km. The Maurienne valley (site **B**) is five times as long as the Chamonix valley. The length of the curved valley is about 80 km. The mountain ridges on both sides reach altitudes of around 3000 m a.s.l. and the width of the valley bottom is about 2 km. Both valleys have sidewalls with slopes of 40°-50°, and have a valley floor that falls in the range of approximately 13-14 m per km.

Radar profiler observation sites are indicated by the letters **A** and **B** in Figure 1. Site **A** is located near the Chamonix valley bottom at an altitude of 1040 m a.s.l. Site **B** is located close to the center of the Maurienne valley at an altitude of 1090 m a.s.l.

## 3. EXPERIMENTAL APPROACH

### 3.1. Equipment

The mobile wind profiler used in the POVA experiment is a 'clean-air' three panel 1238 MHz UHF Doppler radar system designed by Degreane Horizon to measure both wind speed and direction 24 hours a day under all weather conditions. 'Clean air' radars detect irregularities in backscattered signals due to refractive index inhomogeneities caused by turbulence. In the lower troposphere these inhomogeneities are mainly produced by humidity fluctuations. The Doppler shift associated with the turbulence provides a direct measurement of the mean radial velocity along the radar beam. To enable full wind vectors (zonal, meridional and vertical) to be calculated a set of measurements are made in three independent directions. The wind profiler consists of three panels to emit and receive three separate beams one vertical from the central panel and the other two at an elevation of 73° to enable full wind vectors to be calculated. Each panel is an array of eight aerial (antenna) every one being an assembly of

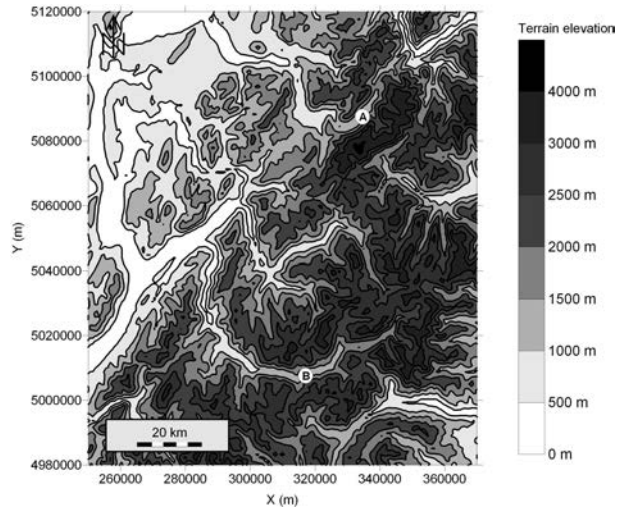


Figure 1: Overview of a part of the Alps with location of the ground based measurements (letter in circles) in UTM coordinate system, zone 32. Colours in the map indicate altitude (see attached colour scale)

eight collinear dipoles. It operates by transmitting electromagnetic energy into the atmosphere and measuring the strength and frequency of backscattered energy. The used mode sampled the boundary layer from 80 m to 3500 m a.g.l. in the vertical, using a 80 m resolution.

Small, portable, tethered balloon data collection system provided experimental data in the lower layers of the atmosphere. The tethered balloon was operated at the same site as the wind profiler in order to document vertical profiles from the ground to the upper atmosphere.

### 3.2. Collection and processing of data

Data were collected from 24 June through July 11, 2003 during the last POVA field campaigns. This study will focus on the whole week of observation in the Maurienne valley from 24 through June 30, 2003. Precipitation event occurred during this week, affecting the quality and the quantity of collected data. Both measurements and numerical simulations were designed for clear weather conditions. As a matter of fact sunny weather alternated with short stormy and rainy periods (see table 1).

Located at *Modane* (**B**), the UHF wind profiler was operated continuously during the entire campaign in order to observe mean and turbulent clear air conditions in the lower atmospheric layer. Data were collected using a three-beam cycle acquired every 6 min. The first three moments were computed with the weighted contiguous spectral lines selected during the last 30 min. The 30-min consensus performs a temporal filter over the considered period removing or smoothing out spurious unwanted echoes.

Vertical tethered balloon soundings of meteorological variables and  $O_3$  in the range of approximately 400-500 m a.g.l. were conducted at *Modane* (**B**), in a quite broad expanse. Vertical sounding operations at each site

Date, June 2003	24		25		26		27		28		29		30
	AM	PM	AM	PM	AM	PM	AM	PM	AM	PM	AM	PM	
Weather conditions	☀	☁	☀	☀	☁	☁	☀	☀	☁	☁	☀	☀	☀
Synoptic wind direction	↗	↗	↗	↗	→	→	→	→	↗	→	↗	↗	↗

Table 1: Weather conditions during the whole week of observation in the Maurienne valley

consisted of deployment of a Tethersonde Meteorological Tower System (TMT)<sup>TM</sup> by Vaisala Inc. with electrochemical concentration cell ozone sonde (Model 4Z ECC-O<sub>3</sub>-Sonde)<sup>TM</sup> by EN-SCI Corporation beneath a 5-m<sup>3</sup> helium-filled balloon and were restricted to daylight hours to meet aircraft safety considerations. Tethersonde flights were intermittent at both sites due to strong winds that halted operations after midday.

### 3.3. Results and discussion

Wind reversal is observed in the morning at 0900 UTC and in the evening at 2000 UTC with the same behavior on every sunny day. Figure 2 illustrates the diurnal changes in the wind direction for June 29, 2003.

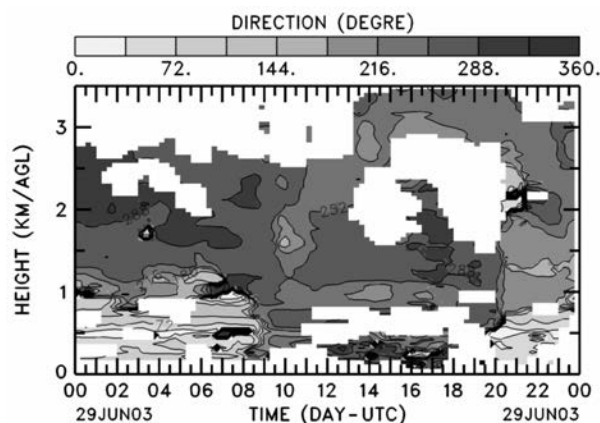
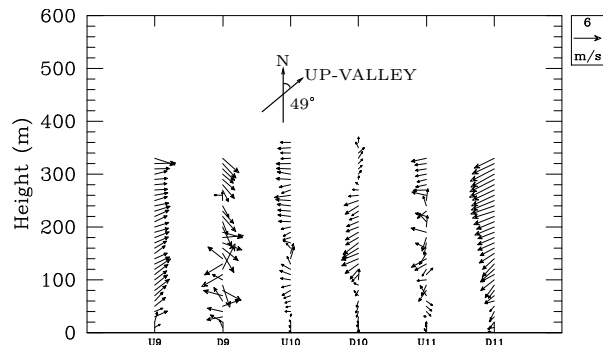
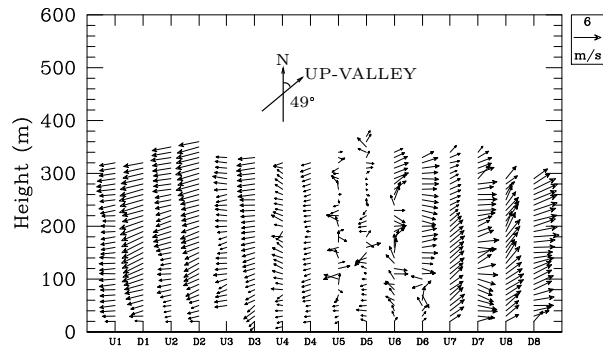


Figure 2: Time-height cross section of horizontal wind direction for June 29, 2003 at Modane in the Maurienne valley

Wind regime changes suddenly across the whole boundary layer instead of gradually proceeding from ground to upper layers as observed in the Chamonix valley. This observation from the tethered balloon at lower layers corroborates the observation from the wind profiler up to about 400-500 m a.g.l. Figure 3 shows wind structure pattern evolution from tethered balloon ascents and descents for June 29, 2003. Except during the rather short transition periods wind direction aligns with the local mean valley direction.

Ozone concentration profiles from tethersonde measurements in figure 4 shows a strong gradient early in the morning which weakens at later time till almost uniform mixing all over the vertical. Ozone increases to a background level which is characteristic of higher altitude

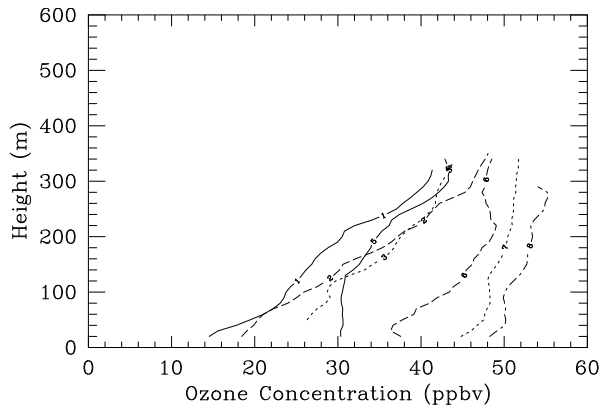


#	Time (UTC)	#	Time (UTC)
1U	0625-0636	7U	1047-1052
1D	0636-0706	7D	1052-1100
2U	0706-0716	8U	1100-1107
2D	0716-0738	8D	1107-1116
3U	0837-0845		
3D	0845-0905		
4U	0933-0942	9U	2038-2043
4D	0942-1008	9D	2043-2109
5U	1008-1019	10U	2109-2117
5D	1019-1026	10D	2117-2126
6U	1026-1034	11U	2126-2134
6D	1034-1047	11D	2134-2143
U (Up)		D (Down)	

Figure 3: Wind structure pattern evolution. Tethered-balloon data, Maurienne valley, June 29, 2003

because of vertical mixing. Therefore ozone is observed to be a good tracer of mixing properties of the flow field. During the morning transition period, ozone concentra-

tion profiles are useful to study the mixed layer structure and its evolution. These profiles are very similar from day to day provided it is a sunny day with predominance of thermally driven wind features.



#	Time (UTC)	#	Time (UTC)
1U	0625-0636	5U	Missing
2U	0706-0716	6U	1026-1034
3U	0837-0845	7U	1047-1052
4U	0933-0942	8U	1100-1107
U (Up)		D (Down)	

Figure 4: Ozone concentration profile evolution. Tethered-balloon data, Maurienne valley, June 29, 2003

## 4. NUMERICAL APPROACH

Large-eddy simulation was used to study meso-scale atmospheric flow fields in both valleys. Small scale modeling is required to take account of the whole frequency range of the fluid motions. The numerical simulations presented in this paper have been conducted with the Advanced Regional Prediction System (ARPS), version 4.5.2. Xue *et al.* (2000, 2001) give an extensive description of the code. Details on the ARPS formulation can also be found at <http://www.caps.ou.edu/ARPS>.

A generalized terrain following coordinate system is used in the ARPS model to solve the non-hydrostatic and compressible Navier-Stokes equation on a staggered Arakawa C-grid. The horizontal grid remains orthogonal while the vertical grid is stretched to follow the terrain, as in the  $\sigma_z$  coordinate system. A coordinate transformation is used to project the terrain-following coordinates to a regular grid in the computational space. The sound wave containing equations are integrated applying a split explicit time integration scheme to accommodate high-frequency acoustic waves. A leapfrog scheme is used to advance advection and diffusion at a large time step. The conservation equation for momentum, heat, mass, water substances, turbulent kinetic energy ( $TKE$ ) and the equation of moist air are solved. The vertical dynamic equation can be solved implicitly.

### 4.1. Physiographic data and grid setup

A good representation of land surface characteristics is necessary for numerical models to reproduce realistically meteorological events and climatological patterns (Marth, 2000). Particular atmospheric phenomena such as blocking of synoptic systems, valley winds and slope winds, can be generated or induced by the topography. The use of realistic and high-resolution topography is required to represent this surface feature. Similarly, the soil-vegetation characteristics are needful for the calculation of surface fluxes of heat, moisture, and momentum over rough surfaces.

Physiographic data sources are provided by Air de l'Ain et des Pays de Savoie (AAPS) and are available with a 100-meter resolution. Data contains orography, roughness, soil type and vegetation type.

The top and bottom boundaries are processed as rigid free-slip boundaries. Surface fluxes are parameterized to take into account the influence of the rough bottom surface. Land-surface energy budget is calculated by a simplified soil-vegetation model (Noilhan and Planton, 1989 ; Pleim and Xiu, 1995). Rayleigh damping was applied to the top one-third of the total domain depth (Xue *et al.*, 2000). Lateral boundary conditions were externally-forced. Lateral boundary values were obtained from the output of larger-scale simulations performed with the Fifth-Generation Penn State/NCAR Mesoscale Model (MM5) version 3 (Grell *et al.*, 1995). MM5 is a non-hydrostatic code which allows meteorological calculation at various scales on a staggered Arakawa B-grid with a two-way nesting technique. The vertical coordinate is a  $\sigma_p$  coordinate what is similar to a terrain following coordinate. In the present study three different domains were used as shown in Table 2.

Typical extent		
Domain 1	France (1500 km)	
Domain 2	Southeastern France (650 km)	
Domain 3	Savoie mountains (350 km)	
Mesh points		Grid size
$n_x$	E-W $\times$ $n_y$	N-S $\Delta x = \Delta y$ (km)
Domain 1	45 $\times$ 51	27
Domain 2	69 $\times$ 63	9
Domain 3	96 $\times$ 96	3

Table 2: Mesh size and dimensions of MM5 domains used for simulations

Boundary conditions of domain 1 was driven by the European Centre for Medium-Range Weather Forecasts (ECMWF) gridded analyses available every 6 hours at 0Z, 6Z, 12Z and 18Z with a horizontal resolution of  $0.5^\circ$  and on 16 pressure levels from 1000 to 50 hPa. In addition the ECMWF first-guesses were used every 6 hours at 3Z, 9Z, 15Z and 21Z to obtain a better temporal description of the synoptic situation. Four Dimensional Variational Analysis (4D-Var) technique was used in the coarser domain to

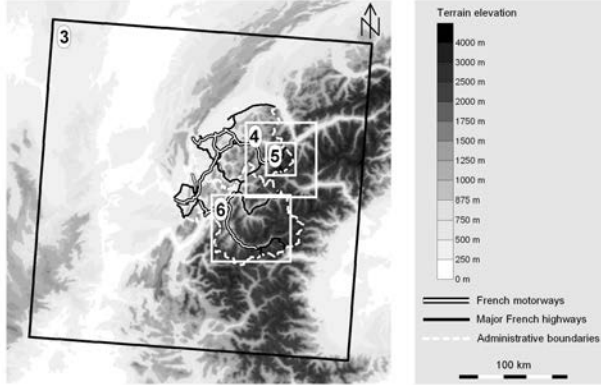


Figure 5: Geographical extents of ARPS domains used for simulations

drive the perturbations needed to control the simulation results (Zou *et al.*, 1997).

Vertically MM5 uses 27 layers with thicknesses ranging from 65 m at the ground to 2 km. The top of the model is at the pressure 100 Pa. The planetary boundary layer (PBL) is described with about 15 layers from 0 to 2000 m a.g.l. with the non-local mixing MRF scheme described by Hong and Pan (1996).

External boundary meteorological fields from the third MM5 domain are applied to ARPS grids using one-way interactive nesting. ‘One-way’ means that the larger grid influences the smaller one, but not vice versa. A relaxation zone similar to that discussed by Davies (1976) was employed to smooth gradients near the lateral boundaries.

For the Chamonix valley modeling with ARPS, two grid nesting levels were used. The first domain is resolved on a 67 E-W by 71 N-S grid with a 1 km horizontal resolution. The grid was chosen to be a one-third reduction in horizontal grid spacing when compared to the third MM5 grid. This run was then further be nested to the final fine grid. The Chamonix valley was resolved on a 93 E-W by 103 N-S grid with spacings of 300 m  $\times$  300 m in the horizontal directions. This grid encompassed a domain of about 25 km  $\times$  25 km. The computation was made on 30 layers. The vertical direction was stretched to accommodate approximately 30 m spacing near the lower wall.

The Maurienne valley was resolved on a 75 E-W by 63 N-S grid with a 1 km resolution. Only one domain is necessary. The lowest layer have a thickness of about 70 m.

Figure 5 and Table 3 give the spatial coverage and the resolution of the different grids used in the presented ARPS simulations.

#### 4.2. Numerical parameters

In the ARPS code, fourth-order horizontal and second-order quadratically conservative differencing scheme was used to solve the momentum and scalar advection terms. Time steps for advection  $\Delta t$  and acoustic modes  $\Delta \tau$  were determined using the Courant-Fredrichs-Levy (CFL) stability condition deduced from minimum vertical grid spac-

Typical extent		
Domain 4	Haute-Savoie Dept. (50 km)	
Domain 5	Chamonix valley (25 km)	
Domain 6	Maurienne valley (100 km)	
Mesh points		Grid size
$n_x$ E-W	$n_y$ N-S	$\Delta x = \Delta y$ (km)
Domain 4	67 $\times$ 71	1
Domain 5	93 $\times$ 103	0.3
Domain 6	75 $\times$ 63	1

Table 3: Mesh size and dimensions of ARPS domains used for simulations

ing and maximum velocity. Practical time step for the fine grid was  $\Delta t = 1$  s and  $\Delta \tau = 0.1$  s. For a typical run on the IBM SP Power4 ‘zahir’ of the Institut du Développement et des Ressources en Informatique Scientifique (IDRIS) on 8 processors with the fine 93  $\times$  103  $\times$  30 grid, the total CPU time per time step per grid point was  $9.40 \times 10^{-6}$ . The code achieved 41.6 Gflops for 8 processors and the memory requirement was a total of 81.6 MB.

The chosen treatment of convective boundary layer turbulence is a combination of the 3D level-1.5 Deardorff subgrid-scale (SGS) scheme and an 1D ensemble turbulence scheme of Sun and Chang (1986). This formulation accounts for the non-local PBL depth instead of the local vertical grid spacing inside an unstable layer to parametrize the local mixing due to SGS turbulence.

Moisture processes were included, but microphysics were disabled since only clear days were simulated. Informations on surface and deep soil temperature predicted by MM5 were used for initialization purpose. Simulation results were particularly sensitive to the surface and deep soil moisture. Their values are chosen so that valley characteristics are close to a typical Alpine valley. During relative dry periods in summer, the volumetric surface and deep soil moistures are about 0.2 m<sup>3</sup> m<sup>-3</sup> (Zappa *et al.*, 2000).

#### 4.3. Results and discussion

Numerical results from the model were compared to measurements for the whole week of observation in the Maurienne valley during summer 2003.

In figure 6, data from the model and *Sainte-Marie-de-Cuines* monitoring station which is typical of a location in the bottom of the valley point out the agreement. Both amplitude and time phase are in agreement. A slight discrepancy at minimal value may be attributed to the difficulties in modeling accurately cooling of lower layer and humidity content of soil canopy at night. No mean drift develops along the whole week of computation time. The spin up from initial condition is rather short (about 2 hours) which may be attributed to the appropriate nesting of boundaries by the models run at larger scales. Similar agreement is observed with wind force and direction, values as low as 1 m/s included (beware of cyclic axis:

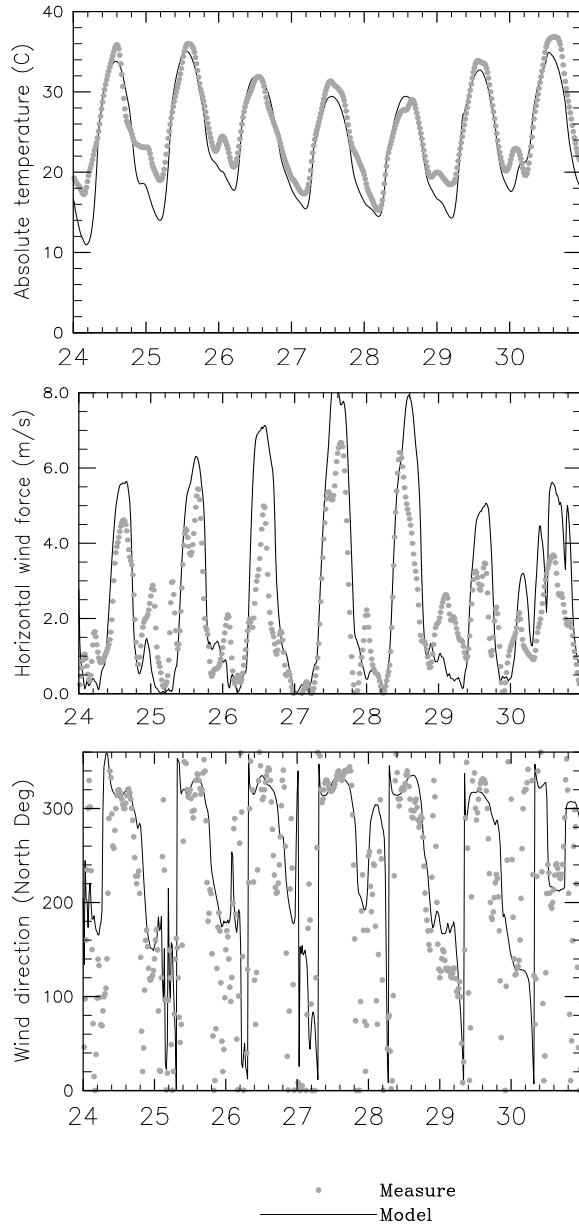


**Figure 6:** *Sainte-Marie-de-Cuines* monitoring station compared to model results for the whole week of field campaign during summer 2003 in the Maurienne valley

$0^\circ = 360^\circ$ ). Scattering of observations is due to inaccuracy of measures at low wind force. Wind direction reverses from down to up in the morning and the opposite at night in accordance with above mentioned tethered balloon data.

Wind direction and force from the wind profiler are compared to corresponding values computed in the model for the whole week of field campaign (see figure 7). The daily periodicity is observed on both wind force and wind direction in spite of a not so good quality of the signal. A lot of sampled data could not be validated

and a perturbation is continuously observed around 500 m a.g.l. because of ground clutter from local orography. Up to about 1000 m a.g.l., the wind reverses twice a day while wind at higher altitude remains unchanged as being driven by large synoptic scales. A mixed layer may be guessed to develop every day up to 1000 m at sunny hours. Particular features may be noticed on June 27, 2003 because of a weather perturbation.

Figure 8 shows isovalues of the vertical velocity  $w$  plotted in valley cross-section along the North direction through *Modane* monitoring station. At 1200 UTC thermal convection develops positive vertical velocities along the slopes up to the summit and negative ones in the middle of the valley resulting into intense vertical mixing.

The hodograph of figure 9a from the model in *Modane* ground station on June 29, 2003 shows that most of the time wind is aligned along the valley axis. It suggests that wind reversal is very sudden as already observed when operating the tethered balloon. It may be compared to the hodograph plotted in *Argentière* ground station in the Chamonix valley (see figure 9b) with a much wider loop. This wider loop may be attributed to slope winds and a more complex topography likely to develop transversal circulation during transition periods.

## 5. SUMMARY & CONCLUSIONS

Wind profiler and tethered balloon were operated to probe vertical flow structure of the atmosphere and its evolution during the last POVA field campaign in summer 2003. At least during this summer field campaign, both valleys exhibit similar behavior such as wind reversal and mixed boundary layer up to approximately the altitude of the surrounding mountains. Nevertheless complex orography makes each valley to develop specific features as illustrated by the hodograph or wind reversal much more sudden in the Maurienne valley than in the Chamonix valley.

Numerical simulations using ARPS were compared with the POVA field data collected during the whole week of field campaign in the Maurienne valley during summer 2003. The simulated meteorological fields are in good agreement with observations. The hierarchy of domains and models succeeds in reproducing realistic dynamical processes in this deep narrow valley. Local thermally driven wind circulation within the valley – up-valley flow during day and down-valley flow during night – was well simulated by the model. Flow fields computed from the model are passed to chemical-transport model in order to assess concentrations of pollutants.

*Acknowledgements.* The research has been supported by the Rhône-Alpes Region, the Agency for Environment and Energy Management (ADEME), the Ministry of Equipment, Transport and Housing (METL) and the Ministry for Ecology and the Durable Development (MEDD). We are grateful to Rémi Dallmayr for assistance with tethered balloon operations. We thank Bernard Campistron for providing us with a listing of his radar postprocessing tool. We also thank Bruno Bénech for a number of very helpful discussions on the tethered balloon device.

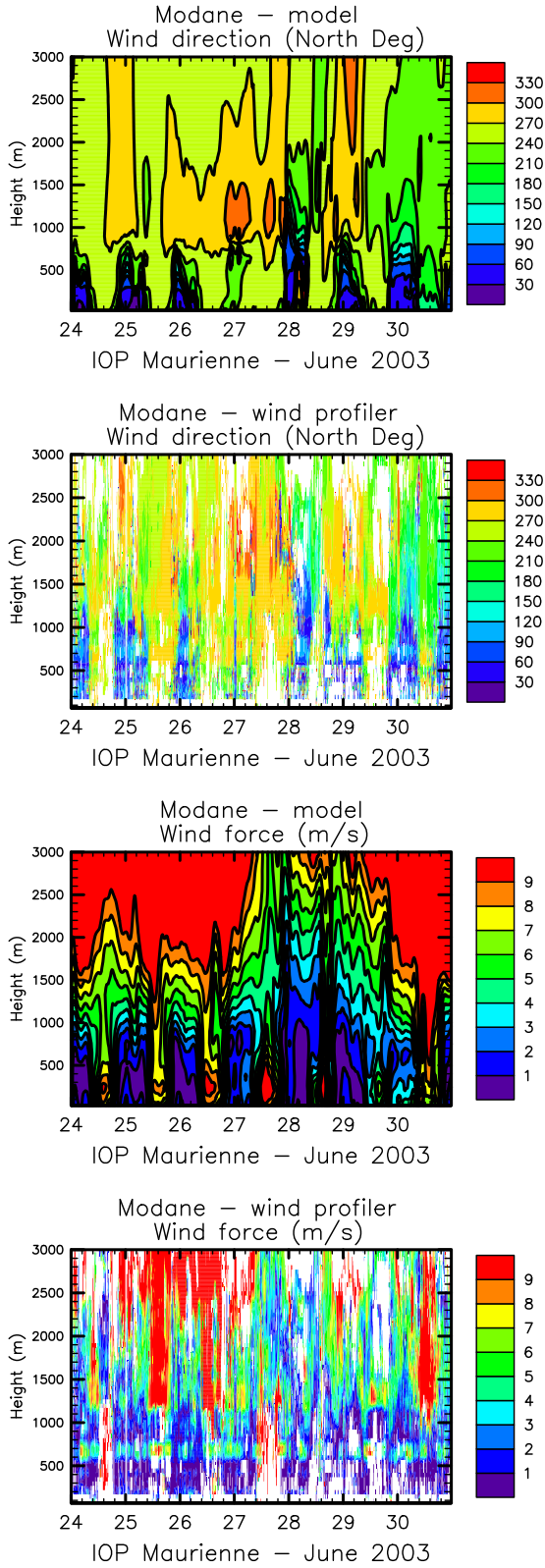


**Figure 7:** Wind structure pattern evolution from ARPS compared to measurements from the wind profiler for the whole week of field campaign during summer 2003 at *Modane* in the Maurienne valley

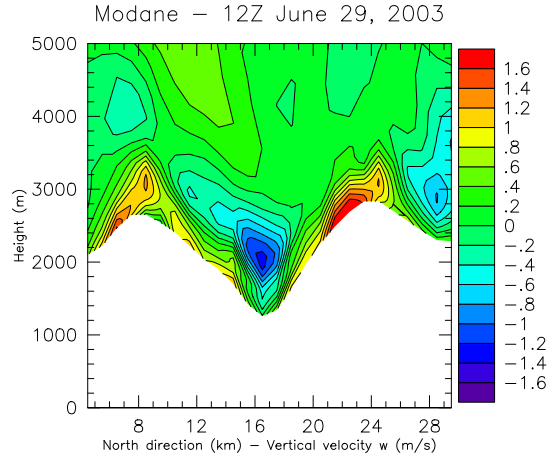


**Figure 8:** Valley cross-section along the North direction through *Modane* monitoring station from the simulation at 1200 UTC on June 29, 2003. Isovalues of  $w$

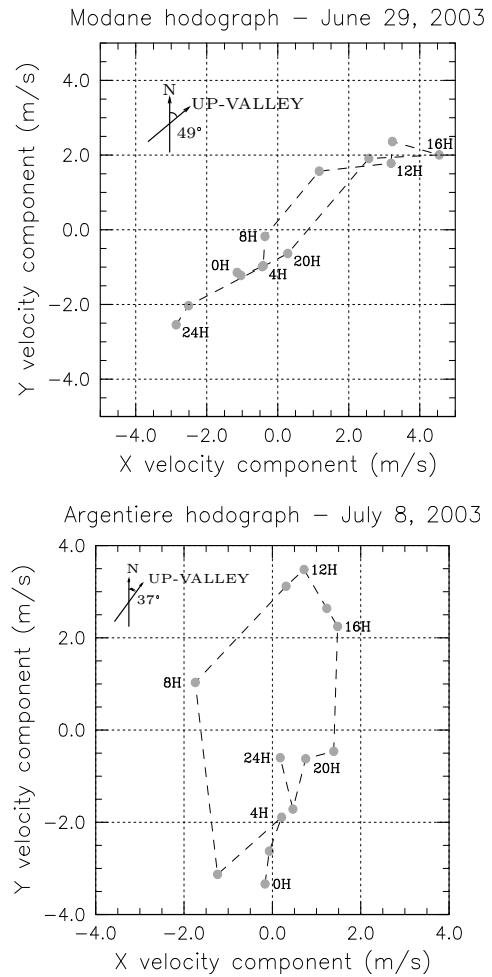


**Figure 9:** Hodograph from the model. (a) *Modane* ground station in the Maurienne valley on June 29, 2003 (b) *Argentiere* ground station in the Chamonix valley on July 8, 2003



## REFERENCES

- Brulfert, G., E. Chaxel, C. Chemel, and J. P. Chollet: 2003, Numerical simulation of air quality in chamonix valley, use of different chemistry indicators. *Proc. of the 14th IUAPPA International Conference Air Quality – Assessment and policy at local, regional and global scales*, Dubrovnik, Croatia, 661–667.
- Chemel, C., J.-P. Chollet, G. Brulfert, and E. Chaxel: 2004, Evolution of convective boundary layer in deep valley for air quality modeling. *Proc. of the 11th Conference on Mountain Meteorology*, Mt. Washington Valley, NH, Amer. Meteor. Soc., [Available on the Amer. Meteor. Soc. website].
- Davies, H. C., 1976: A lateral boundary formulation for multi-level prediction models. *Quart. J. Roy. Met. Soc.*, **102**, 405–418.
- Grell, G. A., J. Dudhia, and D. R. Stauffer, 1995: A description of the fifth-generation penn state/ncar mesoscale model (mm5). NCAR Technical Note NCAR/TN-398+STR, NCAR, Boulder, CO, 117 pp.
- Hong, S. Y. and H. L. Pan, 1996: Nonlocal boundary layer vertical diffusion in a medium-range forecast model. *Mon. Weath. Rev.*, **124**, 2322–2339.
- Marth, L., 2000: Surface heterogeneity and vertical structure of the boundary layer. *Boundary-Layer Meteorol.*, **96**, 33–62.
- Noilhan, J. and S. Planton, 1989: A simple parametrization of land surface processes for meteorological models. *Mon. Weath. Rev.*, **117**, 536–549.
- Pleim, J. E. and A. Xiu, 1995: Development and testing of a surface flux and planetary boundary layer model for application in mesoscale models. *J. Appl. Meteor.*, **34**, 16–32.
- Sun, W. Y. and C. Z. Chang, 1986: Diffusion model for a convective layer. part i: Numerical simulation of convective boundary layer. *J. Climate Appl. Meteor.*, **25**, 1445–1453.
- Whiteman, C. D.: 1990, *Observations of thermally developed wind systems in mountainous terrain*, Amer. Meteor. Soc., Boston, MA, chapter 2 in Atmospheric processes over complex terrain, W. Blumen Ed., Meteorological Monographs, **23**, no. 45. 5–42.
- Xue, M., K. K. Droegemeier, and V. Wong, 2000: The advanced regional prediction system (arps) – a multi-scale non hydrostatic atmospheric simulation and prediction model. part i: Model dynamics and verification. *Met. Atm. Phys.*, **75**, 161–193.
- Xue, M., K. K. Droegemeier, V. Wong, A. Shapiro, K. Brewster, F. Carr, D. Weber, Y. Liu, and D. Wang, 2001: The advanced regional prediction system (arps) – a multi-scale non hydrostatic atmospheric simulation and prediction tool. part ii : Model physics and applications. *Met. Atm. Phys.*, **76**, 143–165.
- Zappa, M., N. Matzinger, and J. Gurtz, 2000: Mesoscale alpine programme (map) hydrological and meteorological measurements at claro (ch) – lago maggiore target area. Technical Report 10(2), Dept. of Civil Engineering, Univ. of Brescia, Italy, 35 pp.
- Zou, X., F. Vandenberghe, M. Pondeva, and Y. H. Kuo, 1997: Introduction to adjoint techniques and the mm5 adjoint modeling system. NCAR Technical Note NCAR/TN-435+STR, NCAR, Boulder, CO, 110 pp.